Quantum Electronics **30** (7) 573 – 579 (2000)

PACS numbers: 33.20.Vq; 34.50.Ez; 42.55.Lt
DOI: 10.1070/QE2000v030n07ABEH001768

Multiquantum vibrational exchange in highly excited CO molecules

A Ionin, Yu M Klimachev, Yu B Konev, A K Kurnosov,
A P Napartovich, D V Sinitsyn, Yu V Terekhov

Abstract. The kinetics of exchange by vibrational quanta is studied theoretically and experimentally in highly excited CO molecules by analysing the recovery time of the inversion population on the selected vibrational-rotational transitions in a doubly *Q*-switched pulsed CO laser. A model of vibrational kinetics that takes into account the multiquantum vibrational exchange between CO molecules in the temperature range between 100 and 300 K is described in detail for the first time. This model is compared with the model of single-quantum vibrational exchange. Good agreement between experimental data and theoretical calculations performed using the model of multiquantum vibrational exchange is the first direct confirmation of the validity of this model.

1. Introduction

The mechanism of population inversion in a CO laser is determined by the energy exchange between molecules in the excited vibrational states. Therefore, to develop a model of such a laser, it is necessary to study the dynamics of the vibrational exchange. The first and the simplest model took into account the exchange by vibrational quanta (the VV exchange) assuming that only one quantum can be transferred in a collision [1]. A set of the rate constants (RCs) for one-quantum processes $CO(v) + CO(u) \rightarrow CO(v-1) + CO(u+1)$ used in calculations was verified experimentally only for lower vibrational levels v and u. The rate constants used for higher vibrational levels were extrapolated from the measured rate constants. Upon extrapolation, the expressions in the first order of the perturbation theory have been used [2 – 5]. However, this procedure was not substantiated physically for calculations of the VV exchange rates in the highly excited CO molecules. In particular, the rate constants determined by this method rapidly increase with increasing quantum numbers v and u and in the case of quasi-resonance exchange they begin to exceed the gas-kinetic values already at small values of v and u (~ 6).

In Ref. [6], more realistic quantum-mechanical numerical calculations of the rates of one-quantum vibrational exchange (OVE) were performed for CO molecules. The calculations of the vibrational distribution function (VDF), i. e., the dependence $N(v)$ of the population on the vibrational level number, with RCs close to those calculated in Ref. [6] proved to be in disagreement with the experiment [7]. This is not surprising, because a decrease in the OVE rate constants at higher levels is compensated by an increase in the RCs of multiquantum vibrational exchange (MVE). The first experimental evidence of a noticeable role of the two-quantum exchange processes in the establishment of the VDF at levels with $v > 15$ has been obtained in experiments on the double resonance in CO [8]. The two-quantum exchange RC estimated in this paper well agrees with the theoretical calculations performed later [9, 10], from which it follows that the m-quantum exchange processes

$$CO(v) + CO(u) \rightarrow CO(v-m) + CO(u+m) \qquad (1)$$

become appreciable when the probabilities of the $(m-1)$-quantum processes are of the order of unity (m is the number of quanta transferred). As shown in Ref. [10], the RCs for processes (1) ($m \geqslant 2$) approach the one-quantum RCs when the vibrational quantum number v exceeds 10.

An analytic theory of the vibrational exchange was developed in [11, 12] and references cited in these papers. This theory can be used to obtain the scaling of the dependence of the RCs on vibrational quantum numbers and temperature based on the exponential dependences of the interaction cross sections on the energy of colliding particles. However, to obtain the parameters of analytic approximations of the interaction cross sections in practice, it is necessary to perform calculations that are similar to those presented in Ref. [10]. As far as we know, such calculations have not been carried out so far.

A kinetic model of a CO laser that takes the MVE into account was developed in Refs [7, 13]. The RCs at the temperature 100 K required for this model that were taken from Refs [9, 10] gave good agreement between the calculated and experimental VDF. However, it was found that the calculated stationary VDF comparatively weakly depends on the approximation chosen for the RC calculation. Calculations [7, 13] also showed that the time evolutions of the VDF after the frequency-selective perturbation, which is typical for the CO laser [8], strongly differ for high vibrational levels

A A Ionin, Yu M Klimachev, D V Sinitsyn, Yu V Terekhov P N Lebedev Physics Institute, Russian Academy of Sciences, Leninskii prospekt 53, 117924 Moscow, Russia
Yu B Konev Institute of High Temperatures, Russian Academy of Sciences, Izhorskaya ul. 13/19, 127412 Moscow, Russia
A K Kurnosov, A P Napartovich Troitsk Institute of Innovative and Thermonuclear Research, 142092 Troitsk, Moscow region, Russia

Received 24 December 1999
Kvantovaya Elektronika **30** (7) 573 – 579 (2000)
Translated by M N Sapozhnikov

($v \approx 25$) in these two models. The method of the double Q-switching in a frequency-selective CO laser proposed in Ref. [14] yielded for the first time the data on the recovery time of the population inversion, which could be compared with calculations. Such a comparison with the model of a CO laser in the OVE approximation [15, 16] showed that the OVE model cannot be applied to the description of the establishment of the VDF for $v \geqslant 14$, and that a more realistic model should be used that takes into account the MVE.

The aim of this study is to verify experimentally a model of the active medium of a CO laser that takes the MVE into account. The MVE model [7, 13] has been formulated for the constant gas temperature.

This precluded a comparison of calculations with experiments. Here, we generalise the MVE model to the case when the gas temperature varied from ~ 100 to 300 K. We verified this MVE model by measuring the recovery time of the second laser pulse energy with respect to the energy of the first pulse upon double Q-switching in a frequency-selective CO laser oscillating on high vibrational transitions.

2. Formulation of the problem and kinetic model of the VV exchange

The OVE model in a CO laser with the $CO-N_2-He$ mixtures was described in detail in Ref. [17]. It contains detailed information on the RCs and all important processes proceeding in the active medium of the CO laser, such as electronic excitation of molecules, the VV exchange between molecules, the vibrational-translational (VT) relaxation, spontaneous and stimulated emission, and spectroscopic data. This information was used in the MVE model without any modifications.

The data presented in a review [18], where the calculations of RCs were generalised and some original papers were considered (for example, [10]), were used for the development of the MVE model. The data for individual processes at the gas mixture temperatures 100, 200, 300, 500, and 1000 K were reported in Ref. [18]. For the three- and four-quantum exchange only a few RCs were presented. We estimated all the elements from a total RC matrix in kinetic equations.

A system of kinetic equations describing the time dependence of the population n_v of CO molecules in the vibrational level v is schematically described by the expression

$$\frac{\mathrm{d}n_v}{\mathrm{d}t} = R^v_{\mathrm{e-V}} + R^v_{\mathrm{VV}} + R^v_{\mathrm{VV'}} + R^v_{\mathrm{VT}} + R^v_{\mathrm{sp}} + R^v_{\mathrm{ind}}, \qquad (2)$$

where $R^v_{\mathrm{e-V}}$, R^v_{VV}, $R^v_{\mathrm{VV'}}$, R^v_{VT}, R^v_{sp}, R^v_{ind} are the rates of electronic excitation of molecules, intra- and intermolecular VV exchange, VT relaxation, and spontaneous and stimulated emission, respectively. More detailed equations are well known (see, for example, [3, 19]), and we do not present them here. The MVE rates are calculated from the expression

$$R^v_{\mathrm{VV}} = \sum_{m \geqslant 1} [W_{v+m,v}\, n_{v+m} + W_{v-m,v}\, n_{v-m} - (W_{v,v+m} + W_{v,v-m}) n_v], \qquad (3)$$

where $W_{v+m,v}$ is the frequency of transitions from the level $v+m$ to the level v and $W_{v-m,v}$ is the frequency of transitions from the level $v-m$ to the level v in processes of the type (1). In turn, the transition frequencies are determined by the expressions

$$W_{v+m,v} = \sum_{i \geqslant m} Q^{i-m,i}_{v+m,v}\, n_{i-m}, \quad W_{v-m,v} = \sum_{i \geqslant m} Q^{v-m,v}_{i,i-m}\, n_i, \qquad (4)$$

where $Q^{i-m,i}_{v+m,v}$ is the RC of the m-quantum exchange. In the case of one-quantum exchange, the summation is performed not only over the vibrational levels of CO but also over the levels of N_2.

For lower vibrational levels, the effect of unharmonicity and, hence, of the MVE is negligible, so that we took the RCs for $v < 5$ from Ref. [17]. Analysis of the data from Ref. [18] allows us to choose the range of v for each number of the quanta being exchanged in which the probability of the multiquantum transitions will be of the order of unity. Processes that fall within this range can be considered as being near-resonance processes, and those that do not fall within this range, as nonresonance processes. All the values of u and v for which the inequality $v - u \geqslant 6$ is satisfied, fall within the nonresonance range.

For near-resonance exothermic processes of the type

$$\mathrm{CO}(v-k) + \mathrm{CO}(v-1) \rightarrow \mathrm{CO}(v-k-1) + \mathrm{CO}(v) \qquad (5)$$

the RC can be represented in the form

$$Q^{v-1,v}_{v-k,v-k-1} = Q^{v-1,v}_{v-1,v-2} \Phi(v,k). \qquad (6)$$

The data presented in Ref. [18] permit the function $\Phi(v,k)$ to be found only for some quantum numbers v. For the rest of $v \leqslant 16$, the function Φ was obtained by a linear extrapolation. For $v > 16$, it was assumed that $\Phi(v,k) = \Phi(16,k)$, because the dependence of Φ on k becomes weak with increasing v. This procedure was applied for calculations of the function Φ at the gas temperatures equal to 100, 200, and 300 K. Hereafter, we will call the RCs calculated by this method the modified RCs (MRCs). We used these MRCs for $v \geqslant 10$. In the range $10 \geqslant v \geqslant 5$, the MRCs for near-resonance processes were calculated using a linear interpolation of the RCs from Refs [17, 18]. The RCs for nonresonance processes were determined by a linear logarithmic interpolation

$$\ln Q^{v,v+1}_{w,w-1} = \ln Q^{v,v+1}_{1,0} + \left(\ln Q^{v,v+1}_{v-5,v-6} - \ln Q^{v,v+1}_{1,0}\right) \frac{w-1}{v-6}, \qquad (7)$$

where $Q^{v,v+1}_{v-5,v-6}$ and $Q^{v,v+1}_{1,0}$ are the RCs from [18] and [17], respectively, and $1 \leqslant w \leqslant v-5$.

For the resonance two-quantum exothermic processes, the data from Ref. [18] allow the function Φ to be determined by the same method as for one-quantum processes. However, the data of Ref. [18] are insufficient for the construction of the function Φ in the case of resonance three- and four-quantum processes. We assumed the RCs for exothermic processes to be independent of the quantum numbers and equal to the corresponding RCs from Ref. [18].

The transition probabilities for nonresonance processes are small. We assumed that their dependence on the quantum numbers corresponds to that obtained from the perturbation theory [20]. The perturbation theory yields the following dependence of the RC on the initial quantum numbers v and u of colliding particles and the number m of quanta being exchanged:

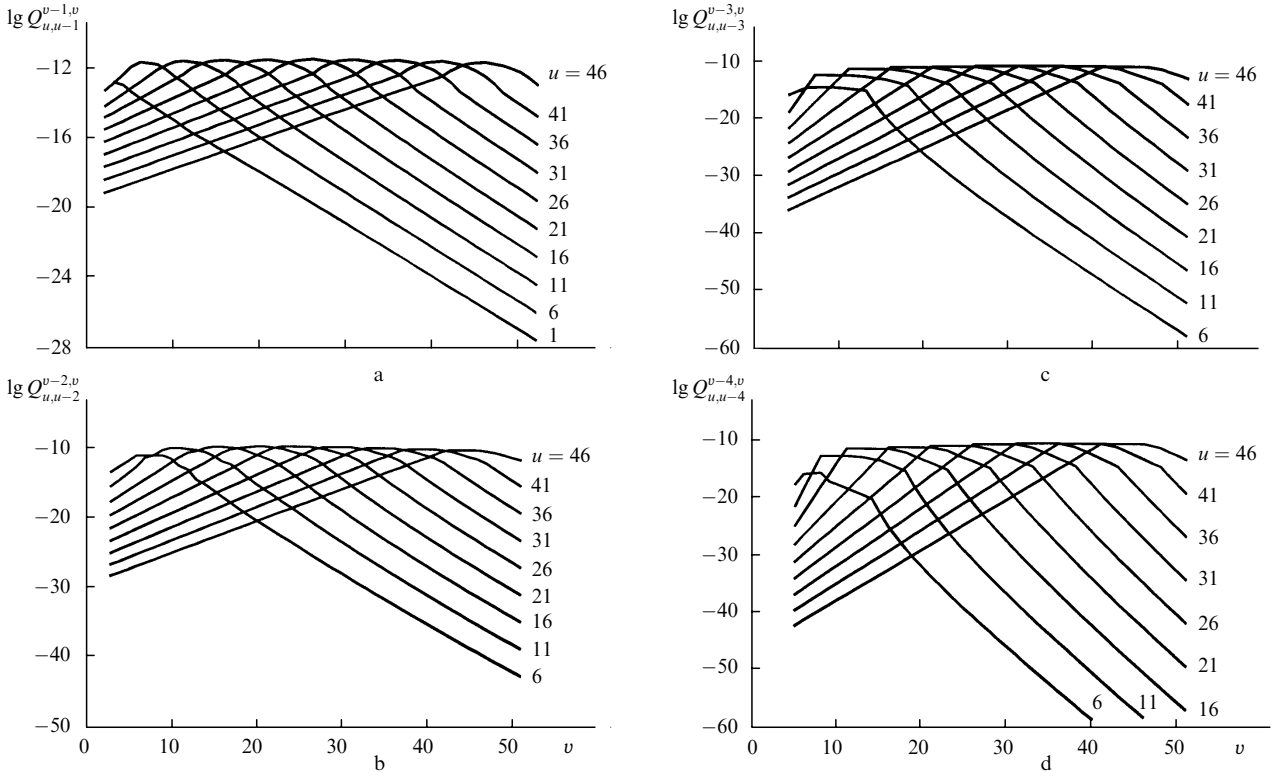

Figure 1. Rate constants of one- (a), two (b), three (c), and four-quantum (d) VV exchange at 100 K.

$$Q^{u,u+m}_{v,v-m} \sim \left|\frac{q_{v,v-m}}{q_{m,0}}\right|^2 \left|\frac{q_{u,u+m}}{q_{0,m}}\right|^2 F\left(\Delta E^{v,v-m}_{u,u+m}\right), \tag{8}$$

where $F(\Delta E)$ is a universal adiabaticity function for nonresonance processes (see, for example, [19]); $\Delta E^{v,v-m}_{u,u+m}$ is the energy defect of a given process; $q_{v,v-m}$ is the matrix element in the lowest order of the perturbation theory, in which an exchange by m quanta is possible. These matrix elements can be calculated using the values of the corresponding Einstein coefficients $A_{v,v'}$ for spontaneous transitions and the transition frequency ν:

$$A_{v,v-m} \sim \left|\frac{q_{v,v-m}}{q_{m,0}}\right|^2 \nu^3_{v,v-m}. \tag{9}$$

The Einstein coefficients $A_{v,v'}$ for transition in the CO molecule are presented, for example, in Ref. [4].

For nonresonance processes, the RCs were normalised by equating them to the RC [18] at the boundary of the resonance range. The MRCs were determined by the above method at 100, 200, and 300 K. Their values at intermediate temperatures were obtained by a linear logarithmic interpolation. The MRCs for endothermic processes were found from the principle of detailed balancing. Fig. 1 shows the MRCs for one-, two-, three-, and four-quantum processes at 100 K, which were used in calculations for comparison with experimental data.

3. Experimental set-up and method

We used in our experiments a cryogenic pulsed Q-switched electroionisation CO laser. The length of the laser active medium was 150 cm and the maximum active volume was 1 litre. The energy, spectral, and temporal parameters of this laser operating on transitions from $3 \rightarrow 2$ to $23 \rightarrow 22$ were studied in detail in Ref. [21].

Fig. 2 shows the optical scheme of the set-up. The laser cavity consisted of the optical system for double Q-switching and a spectral selector, which were located from the opposite sides of the active medium *1*. A laser cell was closed by two flat CaF_2 plates *2* tilted at the Brewster angle to the cavity axis.

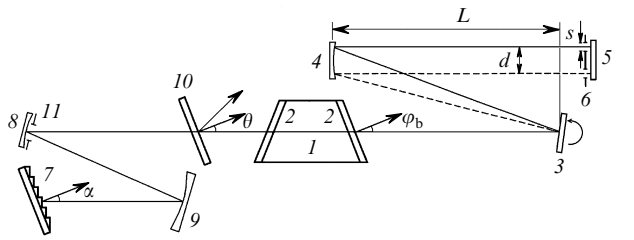

Figure 2. Optical scheme of a spectrally selective double-switched electroionization CO laser:
(*1*) active medium; (*2*) Brewster windows; (*3*) rotating mirror; (*4*, *8*, *9*) totally reflecting spherical mirrors; (*5*) totally reflecting plane mirror; (*6*) optical screen; (*7*) diffraction grating; (*10*) CaF_2 plate outcopler; (*11*) diaphragm.

The optical system for double Q-switching consisted of a plane rotating mirror *3* (the rotational velocity was $V \leqslant 60000$ min^{-1}), a spherical mirror *4* (the radius of curvature was $r = 2$ m), and a plane mirror *5* with an optical screen *6* that controlled the duration and the duty ratio of laser pulses. Rotating mirror *3* was mounted in a focal plane of a spherical mirror *4* (i. e., at the distance $L = r/2$ from it). An opaque screen *6* had two slits in it of width s spaced by the distance d.

The parameters s and d determined, respectively, the duration τ of a single laser pulse and the delay time τ_{1-2} between the first and second pulses. By varying V, s, and d, we could control the temporal parameters of a two-pulsed CO laser: the time τ_{on} (τ_{off}) of switching on (off) of a cavity, τ, and τ_{1-2}. In our experiments, τ_{on} (τ_{off}) and τ were equal to 0.2 and 1.0 μs, respectively. The delay time τ_d between the pump pulse (the pump pulse duration was ~ 40 μs) and the first laser pulse was varied in the range from 200 to 650 μs (Fig. 3).

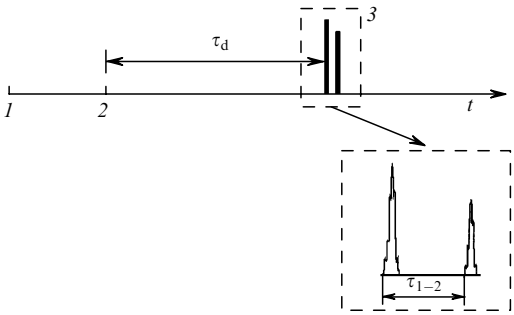

Figure 3. Schematic arrangement of the detected moments and a typical time dependence of the emission intensity of a doubly Q-switched electroionization CO laser: (*1*) Onset of the oscilloscope sweep; (*2*) onset of the pump pulse; (*3*) emission of a doubly Q-switched electroionization CO laser ($\tau_d = 200-650$ μs, $\tau_{1-2} = 1.5-10$ μs).

A spectral selector of the laser cavity was completely independent of the optical double Q-switching system. It contained a 150 litre mm^{-1} diffraction grating *7* with the blaze angle of 26°45′ and an intracavity telescopic beam expander (Fig. 2) consisting of spherical mirrors *8* ($r = 0.5$ m) and *9* ($r = 1.0$ m). On a mirror *8* a diaphragm *11* was mounted of diameter 18 mm. The total cavity length was 6.5 m. The diffraction grating was mounted in an autocollimation scheme. Its resolving power was ~ 5000, corresponding to the spectral resolution of ~ 0.35 cm^{-1} in the wavelength range under study. The angle of incidence α of the laser beam on the diffraction grating was controlled with a relative error of $\sim 0.02\%$, corresponding to the accuracy of the wavelength setting of ± 0.4 cm^{-1}.

Laser emission was extracted from the cavity by reflecting from a plane CaF_2 plate *10* mounted at the angle $\theta = 7°$ to the optical axis. The advantages of this scheme over other spectrally selective schemes of Q-switched IR lasers have been discussed in detail in Ref. [22].

The system for detection of the laser output (not shown in Fig. 2) consisted of an IR detector with a time resolution of $\sim 10^{-9}$ s, a thermoelectric calorimeter with a sensitivity of $\sim 10^{-3}$ J, and an IR spectrograph with a spectral resolution of ~ 0.5 cm^{-1} and the spectral range between 4.5 and 6.5 μm.

The experimental conditions, which were chosen, taking into account the possibility and convenience of comparison of theoretical calculations with experimental results, were as follows. The laser mixture had the composition $CO : N_2 = 1 : 1$, the laser mixture density was $N = 0.047$ Amagat, the initial temperature of the active medium was 100 ± 3 K, and the specific energy input was varied between 270 and 400 J $litre^{-1}$ $Amagat^{-1}$ with an accuracy of 5%.

To compare reliably theoretical calculations with experimental data, it was important to know with good accuracy real optical losses β_0 per round trip in the laser cavity. For this purpose, we measured reflection coefficients of all elements of the laser cavity (except Brewster windows) in the wavelength range from 5.0 to 6.5 μm. The measurement method and the results are reported in Ref. [16].

When comparing the theory with the experiment, we used the ratio $R = Q_2/Q_1$ (where Q_1 and Q_2 are the energies of the first and second laser pulses) to characterise the degree of restoration of the inverse population on the chosen vibrational-rotational transition in the CO molecule. This ratio was obtained for each pair of laser pulses by numerical integration of the corresponding temporal intensity profiles for each pulse with the subsequent normalisation to the total output energy.

Note that we obtained the single-frequency lasing upon double Q-switching on many vibrational-rotational transitions of the vibrational bands from $5 \rightarrow 4$ to $33 \rightarrow 32$. The vibrational-rotational transitions in each vibrational band were separated in accordance with two criteria: (1) The difference between the wavelength of the separated line and those of the nearest lines from the adjacent vibrational bands should be at least two times greater than the resolution of the spectral selector and (2) the separated laser line should fall within the transparency window of the atmosphere and should be only weakly absorbed by water vapour.

The use of the telescopic beam expander resulted in the improvement of the spectral resolution of the spectral selector (~ 0.35 cm^{-1}) compared to that of the scheme used in Ref. [16]. However, total losses in the laser cavity measured by the method described in Ref. [16] remained large ($\sim 40-50\%$). For this reason, the reliable single-frequency lasing was achieved on many vibrational-rotational transitions only near the threshold. However, when we increased the specific energy input into the active medium, the resolving power of the spectral selector was insufficient for providing single-frequency lasing at most of the transitions. As a result, only four vibrational-rotational transitions proved to be acceptable for comparison with the theory, namely, the $13 \rightarrow 12P(11)$, $15 \rightarrow 14P(13)$, $19 \rightarrow 18P(15)$, and $20 \rightarrow 19P(14)$ transitions. The single-frequency lasing on these transitions was observed when the pump energy was considerably greater than the threshold.

For these transitions, we measured peak intensities of a short laser pulse as functions of the delay time τ_d for different energy inputs Q_{in} (Fig. 4). For the values of Q_{in} used, the values of τ_d in the range from 350 to 600 μs correspond to the conditions when the VDF can be considered quasi-stationary. We obtained all experimental results under these conditions

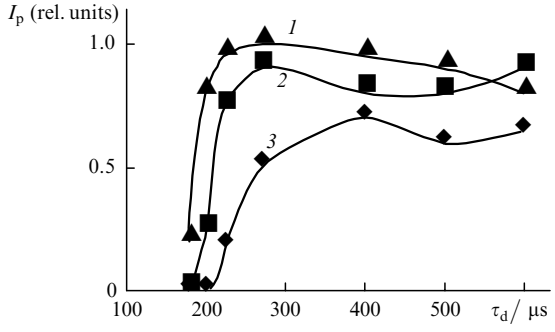

Figure 4. Dependences of the peak intensity I_p of a Q-switched pulsed CO laser on the time delay τ_d for specific energy inputs $Q_{in} = 350$ (*1*), 305 (*2*), and 270 J $litre^{-1}$ $Amagat^{-1}$ (*3*) for the $18 \rightarrow 17P(18)$ transition.

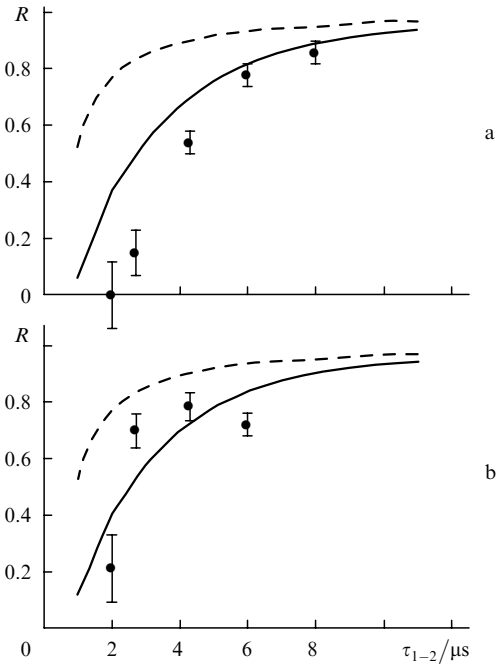

Figure 5. Theoretical (MVE: solid curves, OVE: dashed curves) and experimental (circles) dependences of R on τ_{1-2} for the $13 \rightarrow 12P(11)$ transition for $Q_{in} = 250$ (a) and 290 J litre^{-1} Amagat^{-1} (b); $\tau_d = 590$ μs.

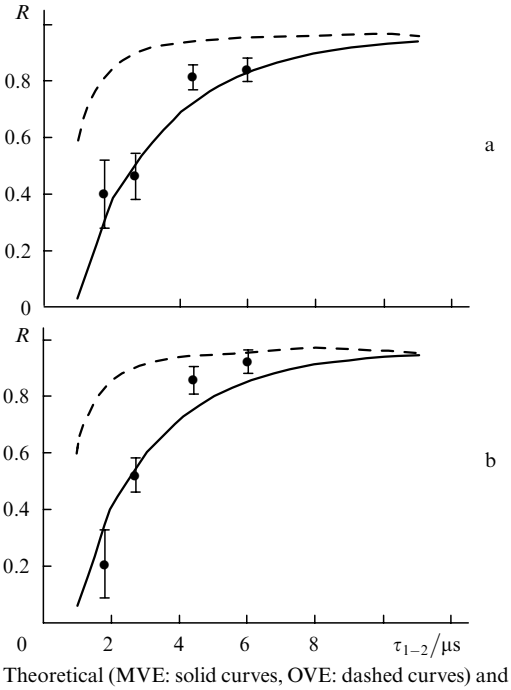

Figure 6. Theoretical (MVE: solid curves, OVE: dashed curves) and experimental (circles) dependences of R on τ_{1-2} for the $15 \rightarrow 14P(13)$ transition for $Q_{in} = 335$ (a) and 375 J litre^{-1} Amagat^{-1} (b); $\tau_d = 590$ μs.

($\tau_d = 350 - 600$ μs, $_{in} = 250 - 560$ J litre^{-1} Amagat^{-1}).

4. Results and discussion

We used in our calculations the same parameters of the active medium (Q_{in}, T, N, the mixture composition, etc.) and laser emission (τ_d, τ, τ_{1-2}, transition wavelengths, etc.), as well as the cavity losses as in experiments. Q-switching was simulated by varying the threshold amplification in

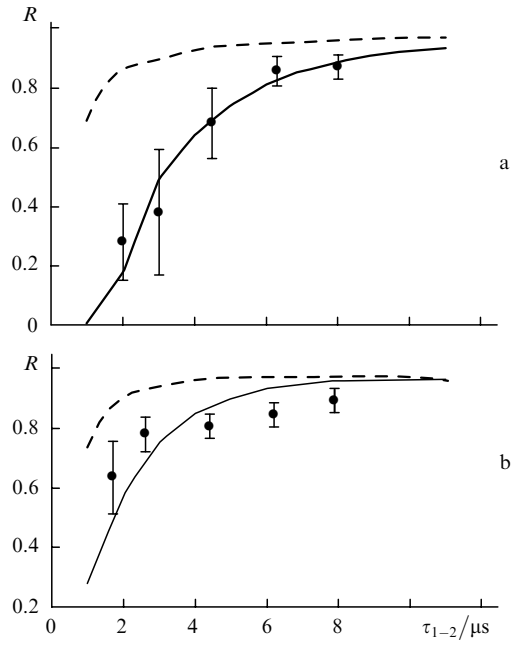

Figure 7. Theoretical (MVE: solid curves, OVE: dashed curves) and experimental (circles) dependences of R on τ_{1-2} for the $19 \rightarrow 18P(15)$ transition for $Q_{in} = 330$ J litre^{-1} Amagat^{-1} (a) and the $20 \rightarrow 19P(14)$ transition for $Q_{in} = 560$ J litre^{-1} Amagat^{-1} (b); $\tau_d = 590$ μs for both transitions.

time. We assumed that it decreased linearly with time for 0.25 μs from the value that exceeded the gain at the selected transition by several times to the preliminary chosen parameter b (the threshold gain), then remained constant for 0.5 μs, and then increased to its initial value for 0.25 μs. Thus, Q-switching occurred for 1 μs. The parameter b corresponded to the cavity losses, which were measured by the method described in Ref. [16].

We calculated R as a function of τ_{1-2} using the kinetic model considered above. The results of our calculations are shown in Figs 5–7 by solid curves. Circles represent the experimental data. We also presented in Figs 5–7 the similar dependences calculated using the OVE model. One can see from Figs 5–7 that the model of the active medium of a CO laser, which takes the MVE into account, describes the experimental results much better than the OVE model. The recovery time of the second laser pulse energy with respect to the first pulse energy is an important parameter of the dynamics of vibrational exchange. Taking into account the fact that in real measurements of the dependences of R on τ_{1-2} (see Figs 5–7) the maximum values of R for different transitions were in the interval between 0.8 and 0.9, this time was determined for the level $R = 0.8$ and was denoted as $\tau_{0.8}$.

The time $\tau_{0.8}$ measured for the transitions under study for the parameters of the active medium and laser emission was in the range from 3.6 to 6.3 μs. In Table 1 are presented the experimental values of $\tau_{0.8}$ and its values calculated using the two models of the vibrational exchange. In our opinion, a great discrepancy between the values of $\tau_{0.8}$ calculated using these two models should be explained. After a short perturbation of the population n_v, it starts to recover according to the equation

$$\frac{d(\Delta n_v)}{dt} \approx -\frac{\Delta n_v}{\tau_{vv}},$$

Table 1. Recovery times $\tau_{0.8}$ of the second pulse energy with respect to the first pulse calculated using the OVE and MVE models and measured experimentally.

Transition ($v \to v-1\ P(J)$)	Q_{in}/J l^{-1} Amagat^{-1}	τ_d/μs	$\tau_{0.8}$/μs		
			OVE	MVE	Experiment
$13 \to 12\ P(11)$	250	590	2.30	5.80	6.3
$13 \to 12\ P(11)$	290	590	2.30	5.30	4.2
$15 \to 14\ P(13)$	330	590	1.70	5.45	4.0
$15 \to 14\ P(13)$	375	590	1.50	5.00	3.6
$19 \to 18\ P(15)$	330	590	1.45	5.80	5.5
$20 \to 19\ P(14)$	560	590	1.30	3.60	3.7

where Δn_v is the population perturbation, τ_{vv} is the VV relaxation time, which, according to (3), is described by the equation

$$\frac{1}{\tau_{vv}} = \sum_{m \geqslant 1} \left(\sum_{i \geqslant 0} n_i Q_{v,v-m}^{i,i+m} + \sum_{i \geqslant m} n_i Q_{i,i-m}^{v,v+m} \right).$$

Fig. 8a shows the dependences of $1/\tau_{vv}$ on the number of the perturbed vibrational level, which were calculated for the typical experimental conditions. One can easily see that for $v > 8$, the frequencies τ_{vv}^{-1} calculated using the MVE model (curve *1*) are noticeably lower than those obtained using the OVE model (curve *2*). For $v > 30$, the frequencies can differ by a factor of five. Curve *3* in Fig. 8a illustrates the contribution of the one-quantum exchange processes to $1/\tau_{vv}$ for the MVE model. The difference between curves *1* and *3* shows that the role of multiquantum processes is quite important. The VDFs calculated with the help of different models at the moment $\tau_d = 590$ μs (under the conditions corresponding to Fig. 8a) are shown in Fig. 8b. Their comparison agrees with the conclusion made in Ref. [7] about a weak sensitivity of the stationary VDF to the choice of the vibrational exchange model.

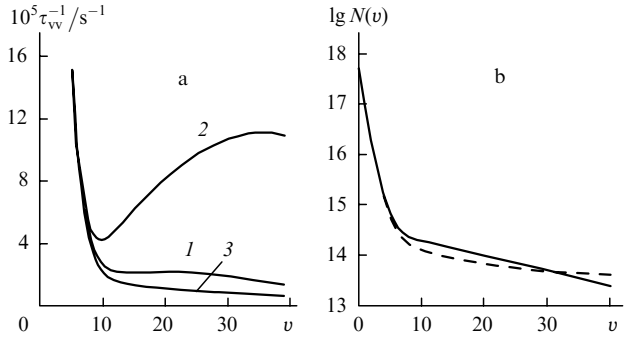

Figure 8. Dependences of $1/\tau_{vv}$ on the number v of the perturbed vibrational level calculated for conditions in Fig. 5a using the MVE (*1*) and OVE (*2*) models. (a) Curve *3* illustrates the one-quantum exchange contribution to $1/\tau_{vv}$ for the MVE model. (b) Logarithmic dependences of the VDF are calculated using the MVE (dashed curve) and OVE (solid curve) models under the same conditions.

Evolution of the VDF in a low-temperature gas excited by a discharge is characterised by two stages. At the first stage, an accumulation of excited molecules on the lower vibrational levels occurs. The duration of this stage is determined by the specific pump power per molecule. When the number of vibrational quanta per molecule becomes critical, the VDF evolution is determined by the vibrational exchange between excited molecules. At this stage, the VDF exhibits a plateau, which results in the appearance of a partial inversion. The duration of the plateau formation is determined by multiple processes of the vibrational exchange, and the rate of the VDF evolution depends on the effective exchange frequencies and the plateau level. The characteristic setting time of a given level of the VDF is approximately proportional to the square of the level number [23], i. e., it is two orders of magnitude longer than the time of exchange by vibrational quanta between molecules on the plateau. In our experiments, this time was a few hundreds of microseconds. The measured time $\tau_{0.8}$ is determined by the vibrational exchange time for molecules on the VDF plateau. Therefore, one should expect that it would be of the order of microseconds, which agrees both with experiments and calculations.

The quantity τ_{vv} plays an important role in the laser kinetics. It allows one to estimate the saturation intensity $I_s/\sigma\tau_{vv}$ upon selective lasing both on the transitions of the fundamental band and on the overtone transitions in the CO molecule ($h\nu$ is a photon emitted at the transition frequency and σ is the induced transition cross section). This important parameter characterises nonlinearity of an active medium with respect to the action of induced radiation.

5. Conclusions

Theoretical and experimental studies of the kinetics of vibrational exchange between highly excited CO molecules allowed us to develop a model of the MVE kinetics in the active medium of a CO laser suggested in Refs [7, 13]. The MVE rate constants, which are required for the theoretical description of the CO laser, were determined by extrapolation and interpolation of the multiquantum exchange RCs known from the literature. The model includes the m-quantum exchange processes ($m = 1, 2, 3, 4$) in the temperature range from 100 to 300 K.

The theoretical MVE calculations are in good agreement with the experimental values of R measured upon selective lasing on several vibrational-rotational transitions in the CO molecule ($v = 13 - 20$), which represents the first direct experimental confirmation of the MVE model.

The double Q-switching method can be used to obtain new information of the VV exchange kinetics. By decreasing the cavity losses, we can advance to the region of higher levels v where the discrepancy between the OVE and MVE calculations is even greater. In this case, it will be possible not only to confirm the validity of the MVE model for the description of the CO laser operation but also to correct the MVE rate constants.

Acknowledgements. This work was supported by the Russian Foundation for Basic Research (Grant No. 99-02-17553), European Office of Aerospace Research and Development, and AF Research Lab. (USA).

References

1. Treanor C H, Rich J W, Rehm R G *J. Chem. Phys.* **48** 1798 (1968)
2. Jeffers W Q, Kelley J D *J. Chem. Phys.* **55** 4433 (1971)
3. Lacina W B, Mann M M, McAllister G H *IEEE J. Quatum Electron.* **9** 588 (1973)
4. Konev Yu B, Kochetov I B, Pevgov V G, et al. *Preprint of Institute of Atomic Energy no. 9* (Moscow, 1977)

5. Smith N S, Hassan H A *AIAA J.* **14** 374 (1976)
6. Dillon T A, Stephenson J C *Phys. Rev. A* **6** 1460 (1972)
7. Konev Yu B, Kochetov I V, Kurnosov A K, et al. *J. Phys. D: Appl. Phys.* **27** 2054 (1994)
8. Brechignac Ph *Chem. Phys.* **34** 119 (1978)
9. Cacciatore M, Billing G D *Chem. Phys.* **58** 395 (1981)
10. Cacciatore M, Billing G D *Chem. Phys. Lett.* **94** 218 (1983)
11. Dubrovskii G V, Bogdanov A V *Chem. Phys. Lett.* **62** 89 (1979)
12. Bogdanov A V, Gorbachev Yu E, Pavlov V A *Preprint of Ioffe Physicotechnical Institute no. 833* (Leningrad, 1983)
13. Konev Yu B, Kochetov I V, Kurnosov A K, et al. *Kvantovaya Elektron. (Moscow)* **21** 133 (1994) [*Quantum Electron.* **24** 124 (1994)]
14. Ionin A A, Klimachev Yu M, Sinitsyn D V, et al. *Proc. SPIE Int. Soc. Opt. Eng.* **3092** 301 (1996)
15. Ionin A A, Klimachev Yu M, Konev Yu B, et al. *Proc. Int. Conf. on LASERS'97* (McLean, VA, STS Press, 1988), pp. 88 – 91
16. Ionin A A, Klimachev Yu M, Konev Yu B, et al. *Izv. Ross. Akad. Nauk, Ser. Fiz.* **63** 676 (1999)
17. Ionin A A, Klimachev Yu M, Kotkov A A, et al. *Preprint of Lebedev Physical Institute no. 11* (Moscow, 1998)
18. Billing G V In: *Nonequilibrium Vibrational Kinetics* (Moscow: Mir, 1989), p. 104
19. Gordiets B F, Osipov A I, Shelepin L A *Kinetic Processes in Gases and Molecular Lasers* (Moscow: Nauka, 1980)
20. Herzfeld K F, Litovitz T A *Absorption and Dispersion of Ultrasonic Waves* (New York: Academic, 1959)
21. Ionin A A, Klimachev Yu M, Kobza G, et al. *Kvantovaya Elektron. (Moscow)* **24** 195 (1997) [*Quantum Electron.* **27** 189 (1997)]
22. Ionin A A, Klimachev Yu M, Kobza G, Sinitsyn D V Patent of the Russian Federation no. 2106731, 12 August, 1996; *Izobreteniya* no. 7 (1998)
23. Zhdanok S A, Napartovich A P, Starostin A N *Zh. Eksp. Teor. Fiz.* **76** 130 (1979)